A mutational analysis of the 5′ *HoxD* genes: dissection of genetic interactions during limb development in the mouse

Allan Peter Davis and Mario R. Capecchi*

Howard Hughes Medical Institute, Department of Human Genetics, University of Utah School of Medicine, Salt Lake City, Utah 84112, USA

*Author for correspondence

SUMMARY

Using gene targeting in mice, we have undertaken a systematic mutational analysis of the homeobox-containing 5′ *HoxD* genes. In particular, we have characterized the limb defects observed in mice with independent targeted disruptions of *hoxd-12* and *hoxd-13*. Animals defective for *hoxd-12* are viable, fertile, and appear outwardly normal yet have minor autopodal defects in the forelimb which include a reduction in the bone length of metacarpals and phalanges, and a malformation of the distal carpal bone d4. The limb phenotypes observed in *hoxd-13* mutant mice are more extensive, including strong reductions in length, complete absences, or improper segmentations of many metacarpal and phalangeal bones. Additionally, the d4 carpal bone is not properly formed and often produces an extra rudimentary digit. To examine the genetic interactions between the 5′ *HoxD* genes, we bred these mutant strains with each other and with our previously characterized *hoxd-11* mouse to produce a series of *trans*-heterozygotes. Skeletal analyses of these mice reveal that these genes interact in the formation of the vertebrate limb, since the

trans-heterozygotes display phenotypes not present in the individual heterozygotes, including more severe carpal, metacarpal and phalangeal defects. Some of these phenotypes appear to be accounted for by a delay in the ossification events in the autopod, which lead to either the failure of fusion or the elimination of cartilaginous elements. Characteristically, these mutations lead to the overall truncation of digits II and V on the forelimb. Additionally, some *trans*-animals show the growth of an extra postaxial digit VI, which is composed of a bony element resembling a phalange. The results demonstrate that these genes interact in the formation of the limb. In addition to the previously characterized paralogous interactions, a multitude of interactions between *Hox* genes is used to finely sculpt the forelimb. The 5′ *Hox* genes could therefore act as a major permissive genetic milieu that has been exploited by evolutionary adaptation to form the tetrapod limbs.

Key words: *HoxD* genes, gene targeting, genetic interaction, limb development, mouse

INTRODUCTION

The vertebrate tetrapod limb has been a favorite system of developmental biologists since the turn of the century because it is dispensable for viability and accessible to experimental manipulation (detailed by Hinchliffe and Johnson, 1980). In addition, the variety in form and function of the limb observed in the extant animal kingdom and the fossil record allows for a merging between the disciplines of genetics, development, and evolution (Hinchliffe, 1994). We are interested in understanding the roles of a set of developmental genes called the *Hox Complex* in the patterning and formation of the vertebrate tetrapod limb.

Hox genes are defined by the presence of a conserved nucleotide sequence (the homeobox) that codes for an amino acid motif (the homeodomain) capable of binding DNA (reviewed by Duboule, 1994). There are at least 39 genes in the mammalian *Hox Complex* that are divided into four linkage groups called HoxA, B, C, and D located on four separate chromosomes. Each locus contains between nine and eleven closely linked individual *Hox* genes forming a genetic matrix believed

to have arisen by a process of chromosomal duplication (Ruddle et al., 1994). Thus, corresponding genes in separate linkage groups are referred to as paralogues since they are most similar to each other in sequence information and expression patterns. The 5′ ends of the Hox loci carry the five paralogous gene families *Hox9-13*. Mutational analysis of some of these genes has demonstrated that they play an important role in limb development (Dollé et al., 1993; Small and Potter, 1993; Davis and Capecchi, 1994; Davis et al., 1995; Favier et al., 1995).

At early stages, the distal tip of the limb bud is composed of rapidly proliferating mesenchymal cells termed the progress zone (PZ), which is covered by a layer of epithelial cells called the apical ectodermal ridge (AER; Tickle and Eichele, 1994). Together these two components maintain each other to allow the limb to grow out of the body in a proximodistal direction (Niswander et al., 1993; Fallon et al., 1994; Cohn et al., 1995; Tabin, 1995). A zone of polarizing activity (ZPA) located at the posterior margin of the limb bud influences the anteroposterior patterning of the limb (Tickle and Eichele, 1994). It is during this early stage of limb bud growth that the *Hox9-13* genes are
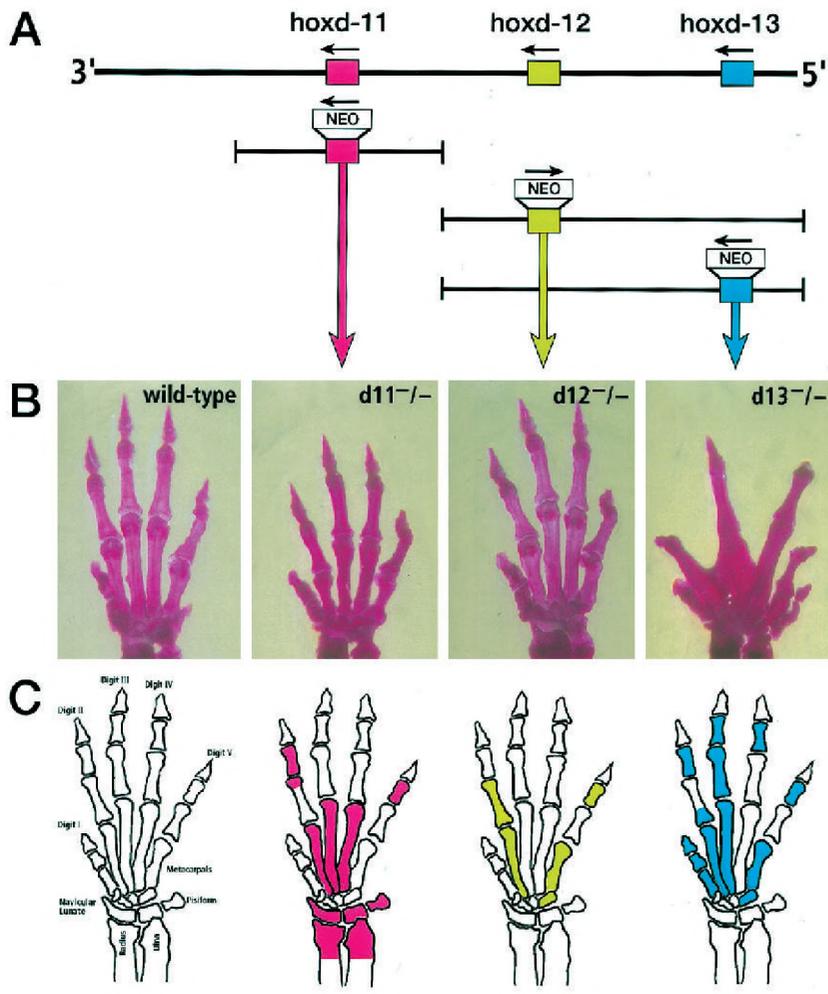
Fig. 1. Targeted mutagenesis of the 5′ *HoxD* genes in mice. (A) Schematic representation of the 5′ end of the *HoxD* locus. The genomic array (top line) is drawn in the 3′ to 5′ direction with the orientation of gene transcription denoted by arrows. The homeobox exons for the respective genes are colored: *hoxd-11* (pink), *hoxd-12* (green) and *hoxd-13* (blue). Three independent gene targeting vectors were constructed (bottom lines) to specifically mutate each gene by the insertion of a disrupting neomycin-resistancy cassette (neo) in the homeobox exon. (B) Dorsal view of the forelimb autopods for a wild-type animal and the three mutant mouse strains produced by gene targeting. The *hoxd-11* mouse has already been described by us (Davis and Capecchi, 1994) and confirmed by others (Favier et al., 1995). The *hoxd-12* mouse is described in this paper. The *hoxd-13* mouse is also reported here and shows identical phenotypes to those described by Dollé et al. (1993). (C) Diagram of a mouse appendicular skeleton and a summary of the sites of the major forelimb phenotypes seen in *hoxd-11* (pink), *hoxd-12* (green) and *hoxd-13* (blue) mutant animals.
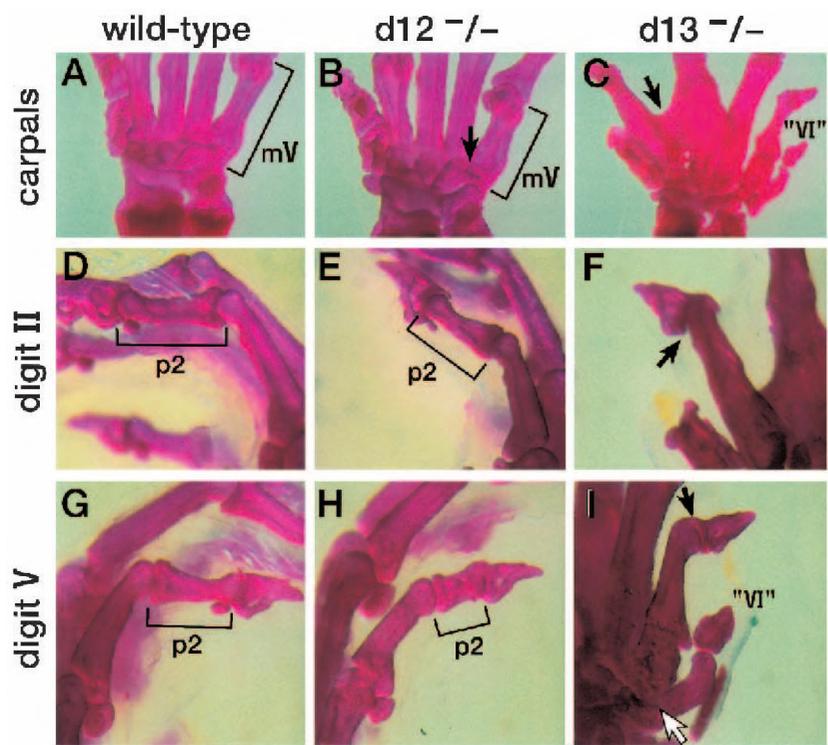

Fig. 2. Phenotypes for *hoxd-12* and *hoxd-13* mutant mice. Autopod of a wild-type forelimb is compared to that of *hoxd-12* and *hoxd-13* mutant animals. The metacarpal of digit V is shorter in *hoxd-12* mice (B) than in controls (A); also, the d4 carpal shows an indentation at its distal border (B, arrow). *Hoxd-13* mice show massive phenotypes including the formation of an extra postaxial digit (C, "VI") and interdigital webbing (C, arrow). Digits II and V in the mutant animals are compromised when compared to controls (D-I). P2 in digit V is reduced in *hoxd-12* animals (H) and is gone in *hoxd-13* mice (I, black arrow). Additionally, in the *hoxd-13* strain, d4 is never properly made and instead yields an extra carpal bone from which grows the postaxial digit VI (I, white arrow).

consecutively activated (Dollé et al., 1989, 1991a,b; Izpisúa-Belmonte et al., 1991). The completed appendicular skeleton is divided into three zones called the stylopod, zeugopod, and autopod. In the forelimb, the stylopod is made up of the humerus, the zeugopod contains both the radius and ulna, and the autopod comprises carpals, metacarpals, and phalanges. These bones are derived from prechondrogenic condensations that are laid down during the early stages of limb growth by cells that have left the PZ. The bifurcation and segmentation of these condensations followed by endochondrial ossification produces the skeletal elements (Shubin and Alberch, 1986).

Hoxd-12 and *hoxd-13* constitute the last two genes of the HoxD locus on Chromosome 2 of the mouse. These genes are activated in a strictly regulated temporal and spatial pattern during development such that the more 3′ gene (*hoxd-12*) is expressed earlier and in a more proximal domain than the more 5′ gene (*hoxd-13*; Duboule, 1992; Izpisúa-Belmonte and Duboule, 1992). This feature of temporal and spatial colinearity of *Hox* genes may play an important role in limb patterning by determining regional identity along the appendicular axis and controlling the properly timed cellular proliferations required for the building of the limb (Davis et al., 1995; Duboule, 1995). To analyze the role of these genes in limb development, we have created targeted disruptions in mice (Capecchi, 1989). Inactivation of *hoxd-12* results in subtle phenotypes restricted to the autopod: specifically, the reduction in length of certain metacarpal and phalangeal bones and the malformation of a distal carpal. The *hoxd-13* mutant mouse, however, displays severe defects of the forepaw including the strong reduction or elimination of certain phalanges and metacarpals, wrist defects, and the growth of a rudimentary postaxial digit.

With only 39 individual genes in the *Hox Complex*, it is believed that these products interact with each other to produce numerous novel combinations that may allow for the vast diversity seen in higher vertebrate body plans. In support of this idea, it has been demonstrated that *Hox* paralogues

function together to specify both the axial and appendicular skeleton of the mouse (Condie and Capecchi, 1994; Davis et al., 1995; Horan et al., 1995). Additionally, it has been shown
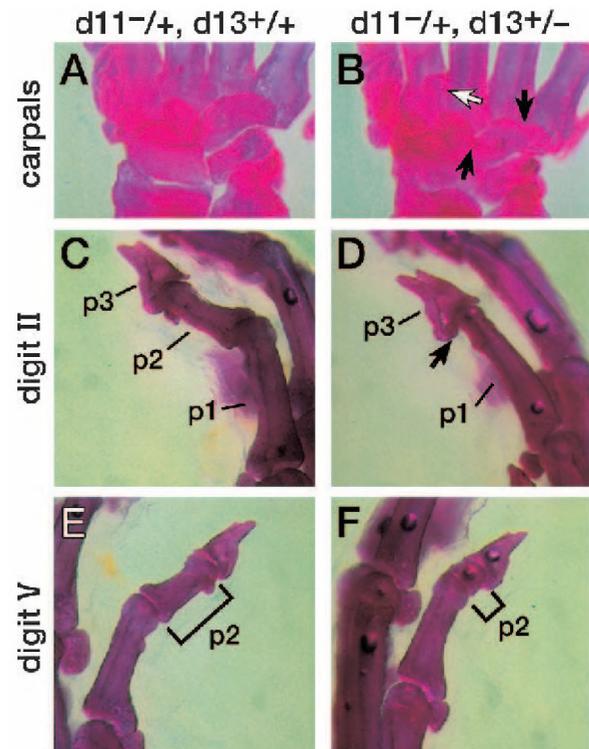

Fig. 3. Limb defects in (*hoxd-11/hoxd-13*) *trans*-heterozygotes. Forelimbs of *trans*-heterozygotes (B) show a bony outgrowth of metacarpal III (white arrow) and the fusion of carpal bones d3 with a malformed (indented) d4 (black arrows) when compared to control heterozygotes (A). P2 of digit II in *trans*-animals (C,D) is often eliminated (black arrow in D), while P2 of digit V is greatly reduced in length (E-F).
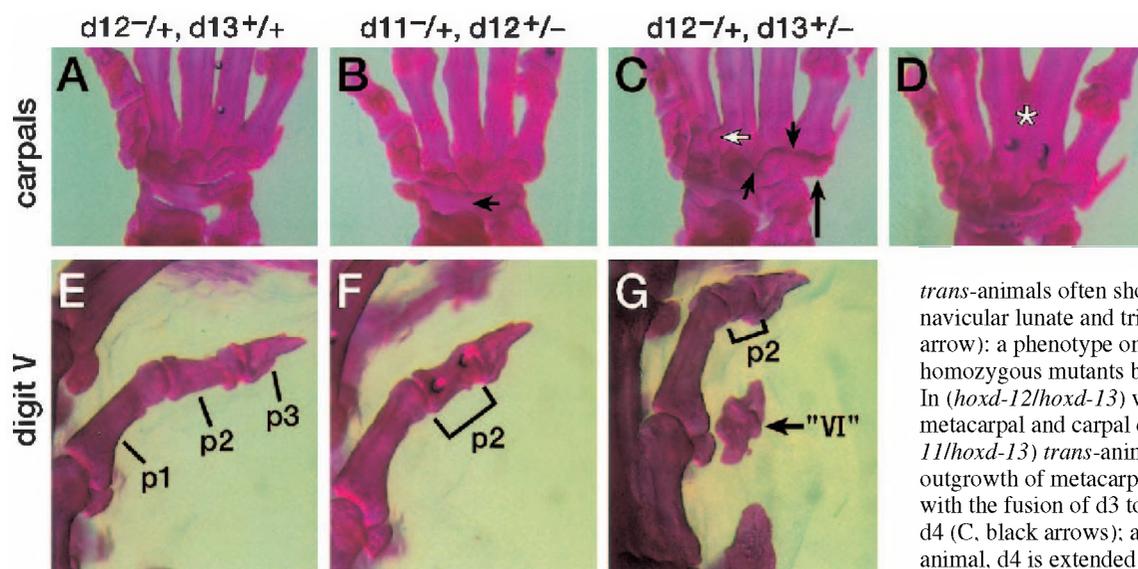

Fig. 4. Limb defects in (*hoxd-11/hoxd-12*) and (*hoxd-12/hoxd-13*) *trans*-heterozygotes. The control is a *hoxd-12* heterozygote littermate (A,E). In the carpal region, (*hoxd-11/hoxd-12*) *trans*-animals often show a fusion between the navicular lunate and triangular carpal bones (B, arrow): a phenotype only seen in *hoxd-11* homozygous mutants but never in *hoxd-12* mice. In (*hoxd-12/hoxd-13*) wrists, the same metacarpal and carpal defects as in (*hoxd-11/hoxd-13*) *trans*-animals is detected: a bony outgrowth of metacarpal III (C, white arrow) with the fusion of d3 to a malformed (indented) d4 (C, black arrows); also note that in this animal, d4 is extended and covers the entire base of metacarpal V (C, long black arrow). Another (*hoxd-12/hoxd-13*) *trans*-littermate shows more severe defects with the large fusion of metacarpals III and IV (D, star). P2 of digit V is reduced in both (*hoxd-11/hoxd-12*) mice (F) and (*hoxd-12/hoxd-13*) *trans*-animals (G). Most noticeably, (*hoxd-12/hoxd-13*) mice are often characterized by the growth of an extra phalange-like postaxial digit (G, "VI").

that *Hox* genes within the same linkage group also work together to control axial patterning (Rancourt et al., 1995). To determine whether genetic interactions within the same linkage group might also control appendicular patterning, we generated a series of mice *trans*-heterozygous for the *hoxd-11*, *hoxd-12*, and *hoxd-13* mutations. These animals show more severe autopodal phenotypes than do the individual heterozygotes, demonstrating a genetic interaction. Finally, we examined the interaction between *hoxa-11* and *hoxd-12* and show that they are required in combination to obtain full outgrowth of the radius and ulna.

MATERIALS AND METHODS

Construction of *hoxd-12* and *hoxd-13* targeting vectors

A DNA fragment that contains both *hoxd-12* and *hoxd-13* was isolated from a genomic library made from mouse CC1.2 embryo-derived stem (ES) cell DNA by using a probe 5′ to the *hoxd-11* locus. The identity of the genes was confirmed by sequencing the homeoboxes (Izpisúa-Belmonte et al., 1991). Replacement-type gene targeting vectors (Thomas and Capecchi, 1987; Thomas et al., 1992; Deng et al., 1993) were constructed individually for *hoxd-12* and *hoxd-13* using the same 12.3 kilobases (kb) of genomic DNA flanked by two *thymidine kinase* genes in a Bluescript-based plasmid. The previously described *neo* expression cassette, KT3NP4 (Davis and Capecchi, 1994), was inserted into the homeodomain of each of the individual genes. For the *hoxd-12* targeting vector, the *XmnI* site in the homeobox was replaced by a *ClaI* linker into which KT3NP4 was inserted in the orientation opposite to that of *hoxd-12* transcription. This site corresponds to amino acid 18 of the homeodomain. For the *hoxd-13* targeting vector, the *PvuII* site in the homeobox was replaced by a *ClaI* linker into which KT3NP4 was inserted in the same orientation as *hoxd-13* transcription. This site corresponds to amino acid 36 of the homeodomain.

Electroporation and ES cell line analysis

The targeting vectors were linearized and electroporated into ES cells. Cell selection and DNA extraction was performed as described (Davis and Capecchi, 1994).

To identify disruption of *hoxd-12*, genomic DNA isolated from individual cell lines was digested with *XhoI* and hybridized with a 1.0 kb *SalI-XhoI* 3′ flanking probe (D). In this case, the wild-type DNA reveals an 8.6 kb DNA fragment and the targeted DNA reveals an extra 5.3 kb DNA fragment. Targeted cell lines were also confirmed by Southern analysis using a *NotI* digest followed by hybridization with a *neo*-specific probe, which reveals an 18 kb band unique to targeted cell lines, a *ClaI* digest hybridized with a 0.3 kb *EcoRI-XhoI* 5′ flanking probe (Z) to detect a band shift from 25 kb (wild-type) to 19 kb (mutant), and a *NotI* + *ClaI* double digest hybridized with two independent internal probes: 1.0 kb *EcoRV-XhoI* fragment (probe N) to detect a band shift from 14 kb (wild-type) to 8 kb (mutant) and a 3.4 kb *XbaI-SalI* fragment (probe C) to detect a band shift from 14 kb (wild-type) to 6.3 kb (mutant).

For *hoxd-13*, cell line genomic DNA was digested with *EcoRV* in a primary screen and hybridized with the 5′ flanking probe Z to detect a band shift from 6.2 kb (wild-type) to 4.5 kb (mutant). Targeted cell lines were confirmed with an *EcoRI* digest hybridized with a *neo*-specific probe to detect a unique 5.5 kb band in targeted cell lines only, a *NotI* digest hybridized with a *neo*-specific probe to detect a unique 18 kb band in targeted cell lines only, and a *ClaI* digest hybridized with the 3′ flanking probe C to detect a band shift of 25 kb (wild-type) to 6.3 kb (mutant).

Breeding, genotyping and skeletal analysis

Mice that carry the targeted mutations were obtained by injection of the appropriate ES cell lines into C57BL/6J (B6) blastocysts. Germline transmission of the mutant alleles from chimeras was confirmed by Southern analysis, and individual breeding colonies were established for the *hoxd-12* and *hoxd-13* mutants. The *hoxa-11* and *hoxd-11* mutations have been described previously (Small and Potter, 1993; Davis and Capecchi, 1994). Genotypes were determined by PCR analysis of tail DNA. PCR was performed in 12.5 µl reactions amplified for 25 cycles at 94°C (30 seconds), 60°C (20 seconds), and 72°C (60 seconds). The *hoxd-11* primers included one that was specific to the intron 5′ of the homeobox (5′ primer) and the other specific to the 3′ untranslated region downstream from the homeobox (3′ primer). The *neo* primer was located at the 5′ end of the KT3NP4 cassette. The *hoxd-12* and *hoxd-13* primers were similarly designed with a 5′ primer and a 3′ primer. The oligonucleotide sequences are provided:

  hoxd-11 5′ primer: 5′-CCTTTTTCCTATCTCAGTGCCAG-3′;
  hoxd-11 3′ primer: 5′-GGGGTACATCCTGGAGTTCTCA-3′;
  hoxd-12 5′ primer: 5′-AGTTGATCTGAGCGAGCTGACAT-3′;
  hoxd-12 3′ primer: 5′-CTTGGTCCAAAAGGGCAGGCTT-3′;
  hoxd-13 5′ primer: 5′-GCTTAGGTGTTCCAAGTATCCAG-3′;
  hoxd-13 3′ primer: 5′-CCACATCAGGAGACAGTGTCTTT-3′;
and
  KT3NP4 *neo* primer: 5′-TTCAAGCCCAAGCTTTCGCGAG-3′.

The PCR products were analyzed using Trevi-Gel agarose electrophoresis. For *hoxd-11*, the products are 507 bp (wild-type) and 367 bp (mutant); for *hoxd-12*: 334 bp (wild-type) and 226 bp (mutant); and for *hoxd-13*: 311 bp (wild-type) and 235 bp (mutant).

For adult skeletal analysis, mice were collected at 7-12 weeks of age and stained with alizarin red. Skeletons of newborn mice were stained with both alizarin red S and alcian blue 8GX. Embryos from timed pregnancies were stained with alcian blue only. All staining and bone length measurements were done as previously described (Condie and Capecchi, 1994; Davis and Capecchi, 1994).

RESULTS

Creating *hoxd-12* and *hoxd-13* mice

Replacement-type gene targeting vectors were constructed by insertion of a *neo*-resistance cassette into the homeodomain-encoding exon of *hoxd-12* and *hoxd-13* respectively (Fig. 1A; Materials and Methods for details). The vectors were independently electroporated into ES cells and cultured under conditions that enrich for homologous recombination events (Mansour et al., 1988). Genomic DNA was isolated from selected cells and characterized by Southern blotting to confirm a targeting event for each gene (Materials and Methods for details). A representative targeted ES cell line for each mutation was injected into B6-derived blastocysts to produce chimeric males that passed the mutation through the germline. All subsequent progeny were confirmed by Southern blotting or PCR analysis using tail DNA, and independent breeding colonies were established for each mutant strain.

Phenotypes of *hoxd-12* and *hoxd-13* mice

Mice heterozygous for *hoxd-12* were intercrossed to produce homozygous mutant animals. This mutation was not lethal as the ratio of genotypes observed in adult mice fulfilled the Mendelian expectation. Homozygous mutants of both sexes were fertile and showed no outwardly apparent abnormalities. However, alizarin red stained skeleton preparations revealed subtle malformations in the forelimb. Defects include reductions in the length of several autopodal bones. The metacarpals of digits II and V are shortened (Table 1 and Fig. 2A,B). Phalange 1 (P1) of digit II is slightly diminished in length (80%

normal bone length) while P2 of digit V is the most strongly affected (55% normal bone length; Table 1 and Fig. 2G,H). Thus, digits II and V appear significantly shorter than control limbs (Table 1). In addition, the wrist carpal bone d4 shows a subtle, characteristic indentation at its distal border (Fig. 2A,B) that could be the result of improper fusion of the prechondrogenic condensations (discussed below). The autopods of mice heterozygous for *hoxd-12* appear normal except for the appearance at low penetrance (approx. 6%) of a very small bony element located postaxially to digit V (not shown).

In contrast, mutations in *hoxd-13* cause extensive limb defects when homozygous. This phenotype has been previously described (Dollé et al., 1993), and the mutant animals reported here show an identical phenotype. Appendicular skeleton defects include a strong diminution of the metacarpal length and the reduction or absence of P2 on digits II and V (Fig. 2F,I). Phalangeal bones on other digits are also shortened due to the failure of normal segmentation. Additionally, a webbed effect is sometimes seen when bony elements fuse the interdigital regions (Fig. 2C). In the wrist, the prechondrogenic condensations that normally fuse together to form the d4 carpal bone fail to do so, yielding an extra wrist bone that often articulates with a rudimentary digit VI (Fig. 2I). Minor carpal defects in d4 (including the indentation) and the same type of postaxial bone as found in *hoxd-12* heterozygotes are seen in *hoxd-13* heterozygotes at a penetrance of 36% (Table 2). The

Table 1. Lengths of mutant forelimb bones, as a percentage of control

Hox Genotype	Control	Bone	Digit II	Digit III	Digit IV	Digit V
d-12 (−/−)	*hoxd-12 (+/+)*	Phalange 2	86	85	94	**55**
		Phalange 1	**80**	90	85	86
		Metacarpal	**78**	91	88	**82**
		Total	81	89	88	77
{d-11 (−/+), d-13 (+/−)}	*hoxd-11 (−/+), hoxd-13 (+/+)*	Phalange 2	**0/65***	91	**82**	**33**
		Phalange 1	93	92	90	90
		Metacarpal	**80**	98	97	95
		Total	**75**	95	92	**79**
{d-11 (−/+), d-12 (+/−)}	*hoxd-12 (−/+), hoxd-13 (+/+)*	Phalange 2	85	89	**83**	**60**
		Phalange 1	**79**	88	88	87
		Metacarpal	**79**	**83**	86	86
		Total	**80**	86	86	**81**
{d-12 (−/+), d-13 (+/−)}	*hoxd-12 (−/+), hoxd-13 (+/+)*	Phalange 2	**81**	86	85	**0/55†**
		Phalange 1	**84**	94	93	93
		Metacarpal	85	102	98	89
		Total	**84**	96	93	**77**

Numbers in **bold** represent strongest reduction in size (greater than 3 standard deviations, where s.d. = ±5% bone length).
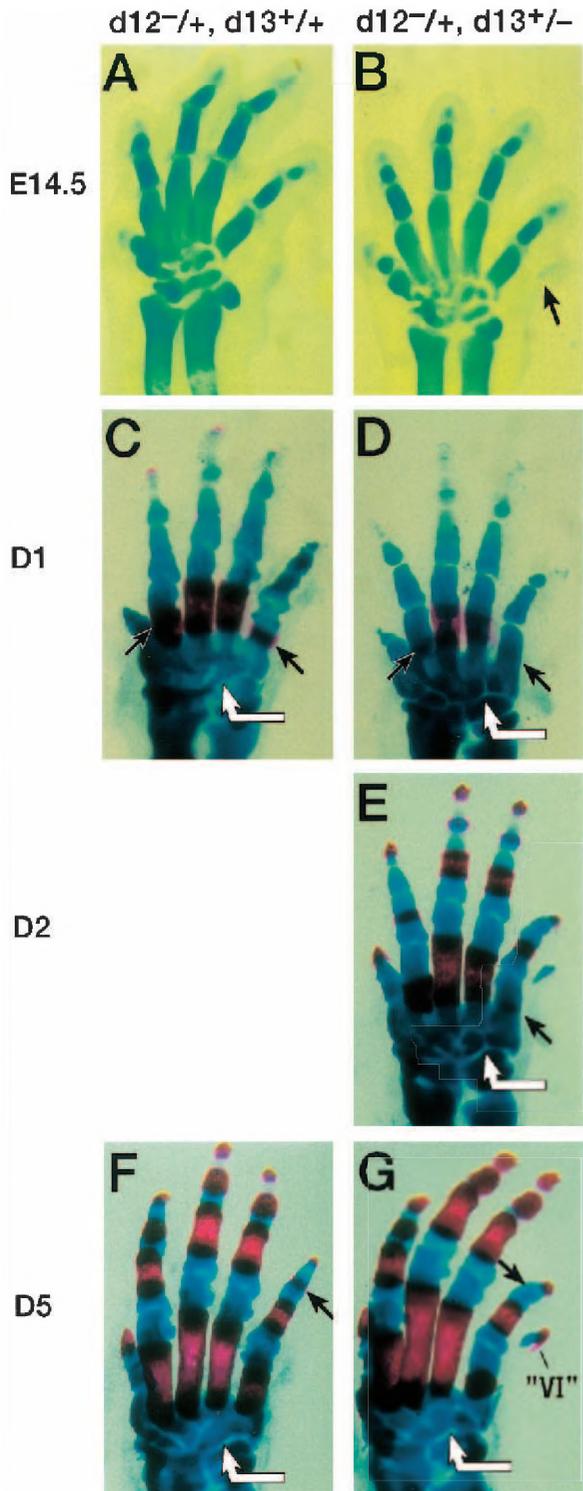*Variable expressivity from 0 to 65%.
†Variable expressivity from 0 to 55%.
Digit I and Phalange 3 are not included since they proved to be un-informative.

Table 2. Summary of limb defects in *trans*-heterozygotes

Hox Genotype	Wild-Type	II:P2	V:P2	C	M	VI	Frequency (%)†
d-11 (−/+)	X						100
d-12 (−/+)	X						94
						X	6
d-13 (−/+)	X						64
						X	18
						X	6
				X		X	6
				X	X	X	6
{d-11 (−/+), d-13 (+/−)}		X	X	X			60
		X	X	X	X		20
		X	X				10
			X	X	X		10
{d-11 (−/+), d-12 (+/−)}				X	X		68
			X	X	X		25
				X	X		7
{d-12 (−/+), d-13 (+/−)}		X	X	X		X	54
		X	X	X	X	X	32
		X	X	X	X		14

*Mutant Phenotypes: II:P2, V:P2 (a reduction in the length of P2 on digits II and V, respectively), C (carpal defects, excluding d4 indentation), M (metacarpal defects), VI (postaxial digit VI present).
†Between 16 and 22 limbs were observed for each genotype.

d12⁻/+, d13⁺/+   d12⁻/+, d13⁺/−

E14.5 A B

D1 C D

D2 E

D5 F G "VI"

Fig. 5. Development of defects in (*hoxd-12/hoxd-13*) *trans*-heterozygotes. Timed embryonic and newborn littermates were collected. By E14.5, the *trans*-heterozygotes can be identified by a cellular outgrowth on the postaxial side of digit V. Cartilaginous staining at this time reveals the nucleus of a condensation event occurring in this outgrowth (B, arrow). At day 1 (D1) of birth, *trans*-animals differ from their littermates in ossification patterns. Control animals show ossification centers for all five digits (C, red staining). Especially note the centers for digits II and V (C, black arrows); additionally, in the wrist, the two prechondrogenic condensations have appropriately fused to form d4 which now appears as one large condensation (C, white arrow). *Trans*-animals show delays in all of these events. By D1, digit II has barely initiated its ossification center (compare the size of red staining of digit II in D with control littermate in C), and has no ossification at all in digit V (D, black arrows); also, the prechondrogenic condensations still have not yet fused to form the d4 pattern, but remain separate as two individual units (D, white arrow). (Note that this particular *trans*-heterozygote did not show the formation of the postaxial digit VI, a phenotype that shows incomplete penetrance; Table 2). One full day later, these two carpal condensations still have not completely fused (E, white arrow), yet an ossification center has finally commenced in digit V (black arrow), and the postaxial digit VI is clearly visible. By D5, again the ossification pattern of P2 in digit V of the *trans*-animal lags behind the control littermates (compare black arrows in F and G). Still, d4 has not properly fused resulting in the indentation at its distal border (compare white arrows in F and G). Digit VI has begun ossifying in the *trans*-heterozygote (G).

Analysis of *trans*-heterozygotes

The sites of limb defects in *hoxd-11*, *hoxd-12*, and *hoxd-13* individual mutant mice are summarized in Fig. 1. The absence of any prominent limb abnormalities in *hoxd-12* mutant mice suggested that perhaps another gene of the *Hox Complex* could be compensating for the loss of *hoxd-12*, as has been demonstrated previously for *hoxd-11* (Davis et al., 1995). Since the limb phenotypes seen in *hoxd-11* and *hoxd-13* mutant mice occur in overlapping domains (Fig. 1C), one or both of these genes might compensate for the absence of the *hoxd-12* gene. Ideally one could test this possibility by creating mice doubly mutant for (*hoxd-11/hoxd-12*) and (*hoxd-12/hoxd-13*). However, these types of strains cannot be generated readily by breeding mice that carry the individual mutations because the number of meioses required to generate the appropriate crossovers is prohibitive. Instead, we decided to create mice *trans*-heterozgyous for the *hoxd-11*, *hoxd-12*, and *hoxd-13* mutations to look for additional limb phenotypes not apparent in mice heterozygous for the individual *HoxD* mutations. The appearance of new phenotypes would suggest an interaction between these gene products. For the analysis described below, *trans*-heterozygotes were generated by breeding a female homozygous mutant for one gene with a male heterozygous for the second mutation. The resulting progeny will be an equal distribution of *trans*-heterozygotes and control littermates (single heterozygotes).

(*Hoxd-11/hoxd-13*) *trans*-heterozygotes (*hoxd-11⁻/+*, *hoxd-13⁺/−*) show several severe defects in the autopod. The base of metacarpal III consistently shows a bony outgrowth. Carpal bones d3 and d4 fuse together at their proximal borders, and d4 shows the same indentation seen in *hoxd-12⁻/−* mice (Fig. 3A,B). Digits II and V are shorter than normal due to the absence or strong reduction in length of P2 (Table 1 and Fig. 3C-F). The phenotype of P2 on digit II shows variable expres-
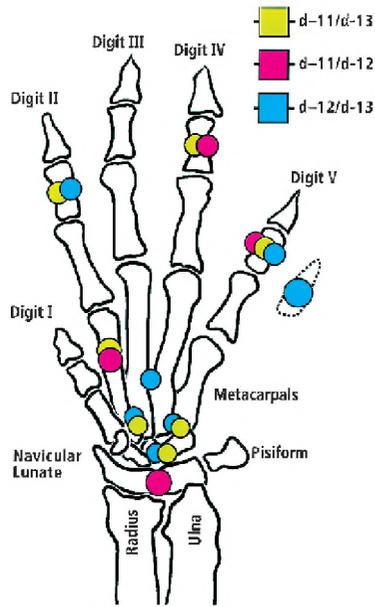
higher penetrance of limb phenotypes in *hoxd-13* heterozygotes with respect to those of *hoxd-12⁻/+* mice (6%) or *hoxd-11⁻/+* mice (0%) is not totally unexpected. If *Hox* gene products function quantitatively to control skeletal patterning, then the dosage of gene products is likely to be an important factor in proper limb formation. Since the homozygous mutant phenotype for *hoxd-13* is more severe than that for *hoxd-11* or *hoxd-12* mutant mice (Fig. 1B), it is not surprising to see a partial phenotype for *hoxd-13* heterozygotes.

Fig. 6. A composite diagram of the limb defects seen in *trans*-heterozygotes. The colored dots represent the physical position of a mutant phenotype when compared to control sibs (see text for details). The figure illustrates several overlapping defects in these three strains including the common phenotypic endpoint of the reduction or elimination of the P2 bone on digits II and V.

Fig. 7. Genetic interaction between *hoxa-11* and *hoxd-12*. The forelimb of a wild-type mouse (A) is compared to that of a *hoxa-11* mutant (B), a *hoxd-12* mutant (C), and the (*hoxa-11/hoxd-12*) double mutant (D). The zeugopod is strongly affected in the double mutant with a sharp curvature in the radius and ulna near the autopodal junction demonstrating a genetic interaction between these nonparalogous *Hox* genes. Six limbs of the double mutant were examined. While this phenotype is 100% penetrant, it does show some variable expressivity in the degree of curvature.

sivity, from total absence of the bone (Fig. 3D) to a strong reduction in its length (Table 1). Overall, these defects lead to the characteristic shortening of digits II and V of the forelimb.

To examine genetic interactions of *hoxd-12* with either *hoxd-11* or *hoxd-13*, we produced both (*hoxd-11/hoxd-12*) *trans*-heterozygotes (*hoxd-11$^{-/+}$*, *hoxd-12$^{+/-}$*) and (*hoxd-12/hoxd-13*) *trans*-heterozygotes (*hoxd-12$^{-/+}$*, *hoxd-13$^{+/-}$*). In the wrist of (*hoxd-11/hoxd-12*) *trans*-animals, a fusion between the navicular lunate and triangular proximal carpal bones is often seen (Fig. 4A,B). This is a phenotype characteristic of *hoxd-11$^{-/-}$* mice, but is never seen in the *hoxd-11$^{-/+}$* heterozygotes (Davis and Capecchi, 1994; Davis et al., 1995). Again, there is a significant reduction in the lengths of specific phalangeal and metacarpal bones that result in the overall truncation of both digits II and V (Table 1) with P2 of digit V showing the greatest reduction in length (Fig. 4E,F).

Lastly, (*hoxd-12/hoxd-13*) *trans*-heterozygotes (*hoxd-12$^{-/+}$*, *hoxd-13$^{+/-}$*) show the strongest interaction of these *HoxD* genes. The wrists of these animals show similar phenotypes to (*hoxd-11/hoxd-13*) *trans*-heterozygotes with a bony outgrowth of metacarpal III, a fusion of d3 and d4 carpal bones at their proximal borders, and the indentation of d4 is sometimes seen (Fig. 4C). Additional phenotypes are also evident. An extension of d4 that covers the entire base of metacarpal V is sometimes seen (Fig. 4C). Another animal had a gross fusion of metacarpals III and IV at their proximal ends (Fig. 4D). The P2 phalange of digits II and V are affected, with digit V having the most severe shortening in this bone (from 0% to 55% of normal P2 length; Table 1 and Fig. 4G). These defects account for the significantly shortened digits II and V relative to controls (Table 1).

Most noticeable in the (*hoxd-12/hoxd-13*) *trans*-heterozygotes, however, is the presence of a rudimentary phalange-like
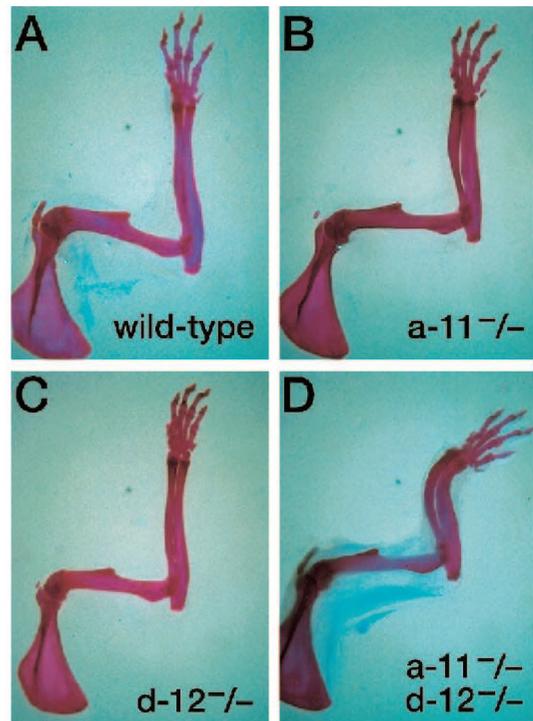
element seen as a postaxial digit VI (Fig. 4G). To follow the development of this bone, we collected timed embryos and newborn pups for skeletal analysis. The sixth digit is readily visible at embryonic day (E)14.5 as a cartilaginous outgrowth on the postaxial side of the forelimb (Fig. 5A,B), but the phalangeal phenotypes are not yet detectable. An extra postaxial bone is sometimes seen in individual *hoxd-12$^{-/+}$* and *hoxd-13$^{-/+}$* heterozygotes. In these cases, however, the phenotype occurs both with a relatively low penetrance (6% for *hoxd-12* heterozygotes and 30% for *hoxd-13* heterozygotes; Table 2) and weak expressivity, where the bone is extremely small and does not resemble the phalange-like element seen in the *trans*-heterozygote mice. In contrast, (*hoxd-12/hoxd-13*) *trans*-animals have the extra digit at 86% penetrance and with stronger expressivity.

Analysis of subsequent developmental time points indicated that the (*hoxd-12/hoxd-13*) *trans*-heterozygotes experience a delay in the ossification events of the autopodal bones. In control littermates, the ossification center for metacarpal V has appeared by day 1 (D1) in newborns, yet in the *trans*-heterozygotes, this same bone does not begin ossification until one full day later (Fig. 5C-E). Similarly by D5 the final limb ossification event at P2 in digit V has been initiated, but is delayed in the *trans*-heterozygotes (Fig. 5F,G). This may account for the severe reduction (and sometimes complete elimination) of P2 on digit V. Additionally, the indentation on the distal carpal

bone d4 may be explained by a delay in the fusion of the two condensations that make up this bone. At D1 it can already be seen that this fusion has taken place in the control littermate, but in the *trans*-animal this growth appears to have been slowed down or delayed such that the two elements remain separate (Fig. 5C-E). By D5, these two condensations approach each other except at their most distal borders which maintain a scalloped outline and lead to the indentation seen in the final ossified bone (Fig. 5G).

Table 2 and Fig. 6 summarize all of the forelimb defects for these *trans*-heterozygous strains. We restricted our analysis to the forelimbs because the hindlimbs showed only mild defects including reductions in the length of P2 on digit V and an aberrant sesamoid bone at the base of metatarsal IV (not shown).

Genetic interaction between *hoxa-11* and *hoxd-12*

Previously we have shown that in mice homozygous for mutations in both *hoxa-11* and *hoxd-11* only a vestige of the radius and ulna are formed (Davis et al., 1995). Since *hoxd-12* does not have a paralogous family member in the HoxA linkage group, we tested for genetic interaction between *hoxa-11* and *hoxd-12*. Mice homozygous for both *hoxa-11* and *hoxd-12* mutations show marked reductions in the length as well as curvature of both the radius and ulna (Fig. 7). *Hoxd-12* mutant homozygotes alone do not have any apparent defect in the formation of the radius and ulna and intermediate genotypes including *hoxa-11, hoxd-12* compound heterozygotes did not show any obvious phenotypes.

DISCUSSION

Mice homozygous for the *hoxd-12* mutation are viable and fertile but show mild defects in the forelimb autopod. In these animals, the lengths of metacarpals in both digits II and V are significantly reduced. In addition, P1 of digit II and P2 of digit V are shorter than normal. Taken together, these phenotypes result in characteristic shortening of digits II and V. In addition, *hoxd-12$^{-/-}$* mice have a subtle defect in the carpal bone d4, which is marked by a reproducible indentation at its distal edge.

Hoxd-13 mutant mice have more extensive phenotypes in the autopod. In these animals, the entire paw is smaller than normal due to the strong reduction, complete absence, or improper segmentation of metacarpal and phalangeal bones in all of the digits, but especially in digits II and V. In the wrist, d4 is not properly formed and instead yields an extra carpal which often produces a rudimentary postaxial digit VI.

Interestingly, the hindlimbs of *hoxd-12* animals appear relatively normal, as was seen for *hoxd-11* mutant mice (Davis and Capecchi, 1994). *Hoxd-13* animals, however, display severe hindlimb defects (not shown here but identical to those reported by Dollé et al., 1993). This difference suggests that the various *HoxD* genes function independently in the different limbs.

The relatively mild forelimb defects seen in *hoxd-12* mice suggested that compensation by other *Hox* genes may be masking this genetic lesion. The notion of spatial and temporal colinearity would have predicted a *hoxd-12* phenotype located between the sites showing a phenotype in *hoxd-11* and *hoxd-*

13 mice (Davis and Capecchi, 1994; Dollé et al., 1993). However, since mutations in *hoxd-11* and *hoxd-13* show overlapping defects (Fig. 1C), it remains possible that either one or both of these genes' products could provide sufficient compensation to allow the near normal development of the forelimb autopod in mice deficient for *hoxd-12*. Genetic redundancy and interaction within the *Hox Complex* have been demonstrated for paralogues involved in the formation of both the axial (Condie and Capecchi, 1994; Horan et al., 1995) and appendicular skeletons (Davis et al., 1995). In addition, nonallelic noncomplementation occurs within the HoxB linkage group during formation of the vertebral column (Rancourt et al., 1995). Here we show, through the analysis of *trans*-heterozygous animals generated from mice mutant for *hoxd-11, hoxd-12* or *hoxd-13*, that adjacent genes of the 5′ *HoxD complex* genetically interact to form the autopod.

The severity of phenotypes in these *trans*-animals increases from (*hoxd-11/hoxd-12*) through (*hoxd-11/hoxd-13*) to (*hoxd-12/hoxd-13*) *trans*-heterozygotes. This pattern seems to reflect a dominant role for *hoxd-13* in the final structure of the autopod. This is not surprising since the *hoxd-13* individual homozygous mutant shows a stronger limb phenotype than that of *hoxd-11* or *hoxd-12* individual mutants (Fig. 1B). From an evolutionary standpoint, this hierarchy may have provided flexibility for modulating the autopod. A limb can be divided into three zones: the most proximal is the stylopod containing one large support bone; this is followed by the middle zeugopod with two similar bones, the radius and ulna, that usually function as a hinge to allow limb rotation; finally at the most distal end is the autopod with several carpal, metacarpal, and phalangeal bones. The most distal end of the limb holds the greatest potential for exploitation by natural selection (e.g., the opposable thumb in primates, the wrist modification in pandas that allows for grasping bamboo, extensive phalangeal growth in bats to produce a large wing, etc.). Thus, it is advantageous to let the last genes (the *Hox-13* cognates) involved in producing the last structures (the autopod) have the greatest developmental dominance in order to influence the autopodal unit. This concept may underlie the phenomenon of 'proximal stability/distal variability' in limb structures (Hinchliffe, 1991).

It is important to note that in all three *trans*-animals we created, the phenotype involves a significant reduction in the total lengths of digits II and V. This is caused primarily by the shortening or total elimination of the P2 bone in each digit. This phenotype is characteristic of numerous *Hox* mutant mice and is consistent with the idea that these genes influence cellular proliferation in limb patterning. Mesenchymal cells form prechondrogenic condensations which subsequently bifurcate and segment to produce a primary pattern of the limb. Because of the ordered development of this primary pattern, a deficiency of limb bud cells invariably causes truncations in the most terminal elements (Shubin and Alberch, 1986). These terminal elements in mice are the P2 bones of digits II and V.

Various secondary modifications of this primary pattern can occur (Muller, 1991). For example, in mice, two wrist condensations fuse together to form the one element that will eventually ossify into the d4 carpal bone. Also, the skeletal analyses of different developmental time points for (*hoxd-12/hoxd-13*) *trans*-heterozygotes demonstrate a delayed timing in ossification events in the autopod, as was seen with *hoxd-13* homozy-

gous mutants (Dollé et al., 1993). This altered timing of development (heterochrony) also occurs in mice mutant for the two paralogues *hoxa-11* and *hoxd-11* (Davis et al., 1995). Thus, it appears that individual mutations in several different *Hox* genes result in a similar defect which could be explained by an insufficient number of cells to finish the autopod (truncating digits II and V by the loss of P2) and a resulting delay in ossification events.

Interestingly, the (*hoxd-12/hoxd-13*) *trans*-animals also produce an extra rudimentary postaxial digit VI that has been observed in other mutant mice (Dollé et al., 1993; Wurst et al., 1994; Lampron et al., 1995; Fawcett et al., 1995) and occurs spontaneously in a partially inbred strain (Cusic and Dagg, 1985). The production of this extra digit is preceded by a local outgrowth of mesenchymal cells on the postaxial side of the limb. The digit, therefore, may be the result of the increased number of mesenchymal cells participating in forming a condensation by overcoming an 'anti-chondrogenic factor' from the overlying ectoderm (Solursh, 1984; Hurle et al., 1991) or by initiating an intrinsic chondrogenic event (Hinchliffe and Horder, 1993). The frequent occurrence of this phenotype in a variety of mice suggests this particular posterior region of the limb bud is very sensitive to cell concentration and/or interaction with the ectoderm (Laufer et al., 1994; Parr and McMahon, 1995; Yang and Niswander, 1995). If *Hox* genes regulate cell proliferation and *Hox*-deficient mice are therefore perceived as having fewer cells to construct a normal limb, then it appears contradictory to have extra digits forming in some of these strains. In addition to regulating the number of limb cells, *Hox* genes may influence other cell properties, such as recruitment and aggregation. Therefore, polydactyly may occur in these strains as a result of the improper distribution of the few remaining limb cells. In support of this, it has recently been reported that *hoxa-13* affects the adhesiveness of limb bud cells by controlling homophilic cell interactions (Yokouchi et al., 1995).

As noted, in (*hoxd-11/hoxd-12*) *trans*-heterozygotes, the phenotypes include an occasional fusion between the navicular lunate and triangular proximal carpal bones. This is an interesting defect because it was initially observed in animals homozygous for a *hoxd-11* mutation (Davis and Capecchi, 1994). Neither *hoxd-11*$^{-/+}$ nor *hoxd-12*$^{-/-}$ animals ever show this phenotype, yet the *trans*-combination of (*hoxd-11*$^{-/+}$, *hoxd-12*$^{+/-}$) is able to reproduce the defect, as if half the amount of the *hoxd-12* gene product can phenocopy the amount of *hoxd-11* gene product from half to zero (i.e., creates a phenotype seen in *hoxd-11* null mice, but not in *hoxd-11* heterozygotes). Mice mutant for the paralogue *hoxa-11* also occasionally show this same fusion, and remarkably, compound heterozygotes between these two *Hox-11* cognate alleles (*hoxa-11*$^{-/+}$; *hoxd-11*$^{-/+}$) also show the phenotype (Davis et al., 1995). From these results we concluded that *hoxa-11* and *hoxd-11* must be working together, since in order to produce this defect all that was required was any two mutant alleles of either *hoxa-11*, *hoxd-11*, or one from each locus. It would appear from this *trans*-heterozygote analysis that *hoxd-11* and *hoxd-12* might also genetically interact in the proper development of the wrist. It is important to note that not every genotype [*hoxa-11*$^{-/-}$ or *hoxd-11*$^{-/-}$ or (*hoxa-11*$^{-/+}$; *hoxd-11*$^{-/+}$) or (*hoxd-11*$^{-/+}$; *hoxd-12*$^{+/-}$)] shows this phenotype with 100% penetrance. This may suggest a degree of variability in the limb patterning

program, where combinations of gene products can compensate, interact, or compete with each other.

Since mutations in *hoxa-11* and *hoxd-11* together almost entirely eliminate the formation of the radius and ulna, and since *hoxd-12* is expressed in the early limb bud after *hoxa-11* and *hoxd-11*, it may appear surprising that combined mutations in *hoxd-12* and *hoxa-11* should affect the length of the radius and ulna above that observed in *hoxa-11* mutant homozygotes alone. A plausible explanation for this observation is that the *Hox-11* paralogous members, which are expressed first and show the most dominant role in the formation of the zeugopod, are involved in initiating the outgrowth of the prechondrogenic condensations that mediate the formation of the radius and ulna. *Hoxd-12* then cooperates with *hoxa-11* and *hoxd-11* (as well as other *Hox* genes) to regulate the final outgrowth of these long bones. This observation again emphasizes the complexity of the genetic interactions among these *Hox* genes in mediating the patterning of the vertebrate limb.

There are seven genetic clues that provide information as to the role of *Hox* genes in limb development. First, individual targeted disruptions of four of the 5′ *Hox* genes (*hoxa-11*, *hoxd-11*, *hoxd-12*, and *hoxd-13*) have not resulted in digit homeosis. Instead, regional malformations in the shapes, lengths and segmentations of bones are observed, suggesting that the *Hox* genes control the localized growth and/or recruitment of cells that contribute to the formation of the appendicular skeleton. Second, these four mutant strains show sites of overlapping limb defects. Third, double mutants for the paralogues *hoxa-11* and *hoxd-11* revealed a major role for *Hox* genes in patterning the limb along the proximodistal axis. In these double mutants, only a vestige of the radius and ulna is formed (Davis et al., 1995). However, following this major discontinuity, limb development resumed. Based on this observation, we proposed that cognate genes of the posterior set of *Hox* genes work in union to specify limb bone formation in the proximal to distal direction. Fourth, nonparalogous as well as paralogous *Hox* genes interact to regulate the final outgrowth of the long bones. A case in point is the shortening and curvature of the radius and ulna in *hoxa-11, hoxd-12* double mutants. The changes in the expression patterns of *Hox* genes during development may account for this genetic interaction. This may result from overlapping expression domains at later developmental time points or by the recruitment of distal cells to interact during the final outgrowth of the limb bones. Fifth, the *trans*-genetic interactions reported here demonstrate that genes in the same linkage group also interact to pattern the limb. Sixth, a characteristic phenotype seen in the majority of these mutant strains is the strong reduction or elimination of P2 in digits II and V, leading to the overall shortening of these two digits. These are the last elements formed in the last digits specified. Such a common endpoint for all of these mutations could be explained if these mutations cause a reduction of cell number at the time of formation of the final elements of the autopod. This observation again emphasizes a common role for these genes in controlling the proliferation of the precursor cells, positively or negatively, needed for forming the limb. Seventh, also common to all of these mutations is a delay in the growth of chondrogenic and ossification patterns. This heterochrony is certainly a major contributor to the final phenotypic consequences of these *Hox* mutations. The observed heterochrony may again result from a shortage of cells.

It is apparent from this genetic analysis that the formation of the vertebrate limb involves a complex set of interactions among multiple *Hox* genes. Due to the extensive overlap of function, the role of individual genes does not become apparent until they are combined with mutations in other members of the complex. A strong role in mediating the proper outgrowth of the limb along the proximodistal axis has been established. What needs to be resolved is how intimately these genes are involved in generating the final pattern of the tetrapod limb. Minimally, these genes appear to play a role in contributing the timed appearance of the precursor cells necessary for limb construction (Davis et al., 1995). However, a more extensive role is likely. Through multiple combinatorial interactions among *Hox* genes, the needed complexity for controlling, positively and negatively, the detailed growth of the limb prechondrogenic condensations could be readily attained. Through such a mechanism the *Hox* genes could be directly responsible for the fine sculpting of the limb bones. In such models the growth and patterning of the limb can be viewed as inherently linked such that the branching and segmentation patterns of the prechondrogenic condensations are a direct consequence of the 'developmental constraints' imposed by the changing limb bud geometry (Oster et al., 1988; Hurle et al., 1991; Hinchliffe and Horder, 1993). We can begin to address such potential roles for *Hox* genes by rearranging the sites and timing of *Hox* gene expression within the context of the native *Hox Complex*. Regardless of the extent of information that *Hox* genes contribute to patterning the limb, they clearly play an influential role in its formation. By varying the timing and expression domains of *Hox* genes in the limb, novel genetic combinations and interactions may have contributed profoundly to the amazing diversity of form and function visible in tetrapod limbs.

REFERENCES

Capecchi, M. R. (1989). Altering the genome by homologous recombination. *Science* 244, 1288-1292.

Cohn, M. J., Izpisúa-Belmonte, J.-C., Abud, H., Heath, J. K. and Tickle, C. (1995). Fibroblast growth factors induce additional limb development from the flank of chick embryos. *Cell* 80, 739-746.

Condie, B. G. and Capecchi, M. R. (1994). Mice with targeted disruptions in the paralogous genes *hoxa-3* and *hoxd-3* reveal synergistic interactions. *Nature* 370, 304-307.

Cusic, A. M. and Dagg, C. P. (1985). Spontaneous and retinoic acid-induced postaxial polydactyly in mice. *Teratology* 31, 49-59.

Davis, A. P. and Capecchi, M. R. (1994). Axial homeosis and appendicular skeleton defects in mice with a targeted disruption of *hoxd-11*. *Development* 120, 2187-2198.

Davis, A. P., Witte, D. P., Hsieh-Li, H. M., Potter, S. S. and Capecchi, M. R. (1995). Absence of radius and ulna in mice lacking *hoxa-11* and *hoxd-11*. *Nature* 375, 791-795.

Deng, C., Thomas, K. R. and Capecchi, M. R. (1993). Location of crossovers during gene targeting with insertion and replacement vectors. *Mol. Cell. Biol.* 13, 2134-2140.

Dollé, P., Dierich, A., LeMeur, M., Schimmang, T., Schuhbaur, B., Chambon, P. and Duboule, D. (1993). Disruption of the *Hoxd-13* gene induces localized heterochrony leading to mice with neotenic limbs. *Cell* 75, 431-441.

Dollé, P., Izpisúa-Belmonte, J. C., Boncinelli, E. and Duboule, D. (1991a). The *Hox-4.8* gene is localized at the 5' extremity of the *Hox-4* complex and is expressed in the most posterior parts of the body during development. *Mech. Dev.* 36, 3-13.

Dollé, P., Izpisúa-Belmonte, J.-C., Brown, J. M., Tickle, C. and Duboule, D. (1991b). *Hox-4* genes and the morphogenesis of mammalian genitalia. *Genes Dev.* 5, 1767-1776.

Dollé, P., Izpisúa-Belmonte, J.-C., Falkenstein, H., Renucci, A. and Duboule, D. (1989). Coordinate expression of the murine *Hox-5* complex homeobox-containing genes during limb pattern formation. *Nature* 342, 767-772.

Duboule, D. (1992). The vertebrate limb: a model system to study the Hox/HOM gene network during development and evolution. *BioEssays* 14, 375-384.

Duboule, D. (1994). *Guidebook to the Homeobox Genes*. New York: Oxford University Press, Inc.

Duboule, D. (1995). Vertebrate *Hox* genes and proliferation: an alternative pathway to homeosis? *Curr. Opin. Genet. Dev.* 5, 525-528.

Fallon, J. F., López, A., Ros, M. A., Savage, M. P., Olwin, B. B. and Simandl, B. K. (1994). FGF-2: Apical ectodermal ridge growth signal for chick limb development. *Science* 264, 104-107.

Favier, B., LeMeur, M., Chambon, P. and Dollé, P. (1995). Axial skeletal homeosis and forelimb malformations in *Hoxd-11* mutant mice. *Proc. Natl. Acad. Sci. USA* 92, 310-314.

Fawcett, D., Pasceri, P., Fraser, R., Colbert, M., Rossant, J. and Giguere, V. (1995). Postaxial polydactyly in forelimbs of *CRABP-II* mutant mice. *Development* 121, 671-679.

Hinchliffe, J. R. (1994). Evolutionary developmental biology of the tetrapod limb. *Development* Supplement, 163-168.

Hinchliffe, J. R. and Horder, T. J. (1993). Lessons from extra digits. In *Limb Development and Regeneration* (ed. J. F. Fallon, P. F. Goetinck, R. O. Kelley and D. L. Stocum) pp. 113-126. New York: John Wiley & Sons, Inc.

Hinchliffe, J. R. and Johnson, D. R. (1980). *The Development of the Vertebrate Limb*. New York: Oxford University Press, Inc.

Hinchliffe, R. (1991). Developmental approaches to the problem of transformation of limb structure in evolution. In *Developmental Patterning of the Vertebrate Limb* (ed. J. R. Hinchliffe, J. M. Hurle and D. Summerbell) pp. 313-323. New York: Plenum Publishing Corp.

Horan, G. S. B., Ramírez-Solis, R., Featherstone, M. S., Wolgemuth, D. J., Bradley, A. and Behringer, R. R. (1995). Compound mutants for the paralogous *hoxa-4*, *hoxb-4*, and *hoxd-4* genes show more complete homeotic transformations and a dose-dependent increase in the number of vertebrae transformed. *Genes Dev.* 9, 1667-1677.

Hurle, J. M., Macias, D., Ganan, Y., Ros, M. A. and Fernandez-Teran, M. A. (1991). The interdigital spaces of the chick leg bud as a model for analysing limb morphogenesis and cell differentiation. In *Developmental Patterning of the Vertebrate Limb* (ed. J. R. Hinchliffe, H. M. Hurle & D. Summerbell) pp. 249-259. New York: Plenum Publishing Corp.

Izpisúa-Belmonte, J.-C., Falkenstein, H., Dollé, P., Renucci, A. and Duboule, D. (1991). Murine genes related to the *Drosophila AbdB* homeotic gene are sequentially expressed during development of the posterior part of the body. *EMBO J.* 10, 2279-2289.

Izpisúa-Belmonte, J. C. and Duboule, D. (1992). Homeobox genes and pattern formation in the vertebrate limb. *Dev. Biol.* 152, 26-36.

Lampron, C., Rochette-Egly, C., Gorry, P., Dollé, P., Mark, M., Lufkin, T., LeMeur, M. and Chambon, P. (1995). Mice deficient in cellular retinoic acid binding protein II (CRABPII) or in both CRABPI and CRABPII are essentially normal. *Development* 121, 539-548.

Laufer, E., Nelson, C. E., Johnson, R. L., Morgan, B. A., and Tabin, C. (1994). *Sonic hedgehog* and *fgf-4* act through a signaling cascade and feedback loop to integrate growth and patterning of the developing limb bud. *Cell* 79, 993-1003.

Mansour, S. L., Thomas, K. R. and Capecchi, M. R. (1988). Disruption of the proto-oncogene *int-2* in mouse embryo-derived stem cells: a general strategy for targeting mutations to non-selectable genes. *Nature* 336, 348-352.

Muller, G. B. (1991). Evolutionary transformation of limb pattern: heterochrony and secondary fusion. In *Developmental Patterning of the Vertebrate Limb* (ed. J. R. Hinchliffe, H. M. Hurle and D. Summerbell) pp. 395-405. New York: Plenum Publishing Corp.

Niswander, L., Tickle, C., Vogel, A., Booth, I. and Martin, G. R. (1993). FGF-4 replaces the apical ectodermal ridge and directs outgrowth and patterning of the limb. *Cell* 75, 579-587.

Oster, G. F., Shubin, N., Murray, J. D. and Alberch, P. (1988). Evolution and morphogenetic rules: the shape of the vertebrate limb in ontogeny and phylogeny. *Evolution* 42, 862-884.

Parr, B. A. and McMahon, A. P. (1995). Dorsalizing signal *Wnt-7a* required for normal polarity of D-V and A-P axes of mouse limb. *Nature* **374**, 350-353.

Rancourt, D. E., Tsuzuki, T. and Capecchi, M. R. (1995). Genetic interaction between *hoxb-5* and *hoxb-6* is revealed by nonallelic noncomplementation. *Genes Dev.* **9**, 108-122.

Ruddle, F. H., Bartels, J. L., Bentley, K. L., Kappen, C., Murtha, M. T. and Pendleton, J. W. (1994). Evolution of *Hox* genes. *Annu. Rev. Genet.* **28**, 423-442.

Shubin, N. H. and Alberch, P. (1986). A morphogenetic approach to the origin and basic organization of the tetrapod limb. *Evol. Biol.* **20**, 319-387.

Small, K. M. and Potter, S. S. (1993). Homeotic transformations and limb defects in *Hoxa-11* mutant mice. *Genes Dev.* **7**, 2318-2328.

Solursh, M. (1984). Ectoderm as a determinant of early tissue pattern in the limb bud. *Cell Differ.* **15**, 17-24.

Tabin, C. J. (1995). The initiation of the limb bud: growth factors, *Hox* genes and retinoids. *Cell* **80**, 671-674.

Thomas, K. R. and Capecchi, M. R. (1987). Site-directed mutagenesis by gene targeting in mouse embryo-derived stem cells. *Cell* **51**, 503-512.

Thomas, K. R., Deng, C. and Capecchi, M. R. (1992). High-fidelity gene targeting in embryonic stem cells by using sequence replacement vectors. *Mol. Cell. Biol.* **12**, 2919-2923.

Tickle, C. and Eichele, G. (1994). Vertebrate limb development. *Annu. Rev. Cell Biol.* **10**, 121-152.

Wurst, V., Auerbach, A. B. and Joyner, A. L. (1994). Multiple developmental defects in *Engrailed-1* mutant mice: an early mid-hindbrain deletion and patterning defects in forelimbs and sternum. *Development* **120**, 2065-2075.

Yang, Y. and Niswander, L. (1995). Interaction between the signaling molecules WNT7a and SHH during vertebrate limb development: dorsal signals regulate anteroposterior patterning. *Cell* **80**, 939-947.

Yokouchi, Y., Nakazato, S., Yamamoto, M., Goto, Y., Kameda, T., Iba, H. and Kuroiwa, A. (1995). Misexpression of *Hoxa-13* induces cartilage homeotic transformation and changes cell adhesiveness in chick limb buds. *Genes Dev.* **9**, 2509-2522.